Int. J. Therm. Sci. (1999) 38, 42–50

Numerical analysis of natural laminar convection in a radial solar heater

Marco Aurelio dos Santos Bernardes [a], Ramon Molina Valle [b], Márcio Fonte-Boa Cortez [b*]

[a] *Department of Mechanical Engineering, CEFET-MAG, Av. Amazonas, 7675, Gameleira, Belo Horizonte, MG, Brazil*
[b] *Department of Mechanical Engineering, Universidade Federal de Minas Gerais, Av. Antônio Carlos, 6627, Pampulha, Belo Horizonte, MG, 31270-901, Brazil*

(Received 30 March 1998, accepted 15 May 1998)

Abstract—This paper presents a theoretical analysis of a Solar Radial Air Heater, operating on natural laminar convection in steady state, to predict the thermo-hydrodynamic behavior of the device. Temperature conditions were imposed on boundaries, so as to limit the flow in the laminar regime along the device. The mathematical model (Navier–Stokes and Energy Equations) was analyzed by the Finite Volumes Method in Generalized Coordinates. The solution was obtained in a fixed computational domain independent of the geometrical shape of the physical system. This methodology allows a detailed visualization of the effects of geometric and operational characteristics for such devices. © Elsevier, Paris

solar chimney / free convection / applied solar energy / renewable energy sources

Résumé — Analyse numérique en convection naturelle laminaire du système radial de chauffage solaire. On présente dans cet article une analyse théorique de ce qu'on appelle «Solar Radial Air Heater» (système radial de chauffage solaire), fonctionnant en convection naturelle laminaire, pour la prédiction du comportement thermo-hydrodynamique du système. Le modèle mathématique (équations de bilan de la quantité de mouvement de l'énergie) a été exploité en utilisant la méthode des volumes finis en coordonnées généralisées. La solution est obtenue pour un domaine de calcul fixé, indépendant de la forme géométrique du système physique. Cette méthodologie permet une visualisation détaillée des effets géométriques sur les champs de vitesse et de température, qui sont très importants pour la définition de la géométrie et des caractéristiques opérationnelles optimales de tels systèmes. © Elsevier, Paris

cheminée solaire / convection libre / énergie solaire appliquée / sources renouvenables d'énergie

Nomenclature

A	finite-difference coefficients	
B	source term	
C_p	specific heat of air	$J \cdot kg^{-1} \cdot K^{-1}$
g	gravitational acceleration	$m \cdot s^{-2}$
H_{c1}	cover height at the junction	m
H_{c2}	cover height at the entrance	m
H_t	chimney height	m
J	Jacobian	
k	thermal conductivity of air	$W \cdot m^{-1} \cdot K^{-1}$
L	length	m
$L[...]$	numerical approximation	
$\dot{M}$	mass flow rate	$kg \cdot s^{-1}$
P	control volume	
p	pressure	
P^ϕ, S^ϕ	source terms	
r,y	coordinates	m
R_c	canopy radius	m
R_{ex}	junction outer radius	m
R_{in}	junction inner radius	m
R_{t1}	chimney lower section radius	m
R_{t2}	chimney upper section radius	m
t	time	s
T_0	ambiant air temperature	K
T_c	canopy temperature	
T_{s1}	ground temperature	K
T_t	chimney temperature	K
u,v,U,V	velocities	$m \cdot s^{-1}$

Greek letters

α, β, γ	metric tensors	
ρ	density of air	$kg \cdot m^{-3}$

* Correspondence and reprints.
fonteboa@vesper.demec.ufmg.br

μ	viscosity of fluid.....	$kg \cdot s^{-1} \cdot m^{-1}$
ν	kinematic viscosity of fluid..	$m^2 \cdot s^{-1}$
η, ξ	generalized coordinates	
ϕ	generic property	
Γ^{ϕ}	diffusivity	
β	volumetric thermal expansion coefficient.....	K^{-1}

Subscripts

e, w, n, s, p	face indicators
P, E, N, S, NE, N, W, SE, SW	point indicators
x, y, ξ, η	partial derivatives

Superscripts

0	previous iteration

1. INTRODUCTION

The Radial Solar System here proposed consists basically of two main components (*figure 1*): the collector (Greenhouse) and the chimney. In this collector system, cold air enters at an end and is heated by solar radiation, flowing confluently along a translucent cover towards the chimney. The flow becomes ascending in the chimney, being driven by buoyancy forces. Such forces, originated by differences of density, cause a strong flow in the chimney, thus making the system workable.

In this system the flow can be used for power generation or for drying. The power generation is obtained by means of an eolic turbine placed at the base of the chimney (solar chimney). This particular subject is not within the scope of study and analysis envisaged by this paper. The drying process is achieved through the warm air flow. In agriculture, warm air can be used for grain drying and fruit dehydration. In industry it can be used in ceramic, paper and cement industries.

The radial solar heater is of simple construction and low cost, as it uses technologies and materials available in Third World countries. Moreover, it has a satisfactory functioning during the night (by storing heat in the ground) and no need for cooling water for the components nor local manpower. Considering its simple constructive and operational characteristics, there is a cost solution and a sensible decrease in its maintenance—there are no mobile components, except in the case of an eolic device [1].

Various global analyses have been developed on this type of system. Such studies comprise calculations of output energy, system efficiency, parametric analyses and analytic models. The results show that this device can be considered as a technically and economically viable form of renewable energy. However, important information is still to be gathered, such as the effect of irregularities in solar radiation, values applicable to real systems, different geometric configurations, characteristics specific to a design as proposed (energy of drying), efficiency and costs. All these details are needed for the design of a working system.

The purpose of this paper is to present a preliminary analysis of the phenomenon of natural convection in a geometry similar to that of the Radial Solar Heater as drawn in *figure 1*, without, however, the eolic turbine. Steady-state laminar natural convection with prescribed boundary condition was considered. This analysis does broach the phenomena of solar radiation and the eolic generator.

To solve the system of equations, the Finite Volumes Method in Generalized Coordinates was used. Velocity and isothermal characteristics of the flow were obtained as functions of the geometry and of the thermal conditions imposed, which makes possible a local analysis and the evaluation of the most appropriate geometric configurations. Local analysis permits the evaluation of local phenomena, which may appear in certain regions. In this way, one can attain even the tiniest details, allowing the achievement of the most adequate design and execution.

2. MATHEMATICAL MODELING

The proposed Radial Solar Heater consists of a lower cylindrical region representing the ground, and a higher disc corresponding to the cover. The cover is coupled at the center with a vertical tube which constitutes the chimney, as in *figure 1*.

The difference of temperature between the interior and the exterior generates a density gradient in the

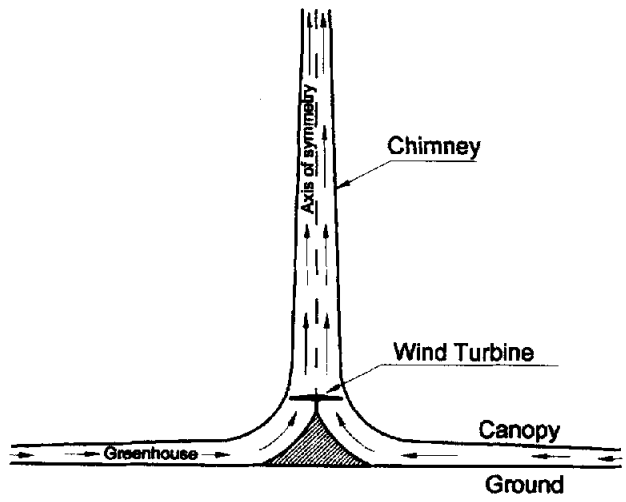

Figure 1. Schematic drawing of an Aero-Solar Radial system.

internal air, thus creating a potential (mechanical) energy within the system. The air heated under the cover enters the chimney at a higher temperature than the atmosphere one, then moving up due to buoyancy forces. Initially, this flow develops in the horizontal direction, which changes to vertical on entering the chimney. The flow section between the cover and the ground reduces its size in the direction of the center of the system, causing the velocities to increase; the maximum value is obtained at the summit of the chimney. As the cover is open at its circumference, the air flows continuously towards the interior of the system, thus guaranteeing its functioning.

The adopted model considered steady state laminar flow and prescribed boundary conditions for temperature and velocity. The hypotheses admitted in this formulation were based on incompressible flow, Newtonian fluid, constant fluid properties, no heat sources, no viscous dissipation, no effect of the solar radiation. The model is constituted by the mass conservation equation, equation of conservation of linear momentum in the r and y directions, equation of energy conservation—and in cylindrical coordinates for an axisymmetric geometry, according to *figure 1*.

Continuity:

$$\frac{\partial \rho}{\partial t} + \frac{1}{r}\frac{\partial}{\partial r}(\rho r u) + \frac{\partial}{\partial y}(\rho v) = 0 \tag{1}$$

Motion – r component:

$$\frac{\partial}{\partial t}(\rho u) + \frac{1}{r}\frac{\partial}{\partial y}(r\rho u u) + \frac{\partial}{\partial u}(\rho v u) = \frac{1}{r}\frac{\partial}{\partial r}\left(r\mu\frac{\partial u}{\partial r}\right) + \frac{\partial}{\partial y}\left(\mu\frac{\partial u}{\partial y}\right) - \frac{\partial p}{\partial r} - \frac{2\mu u}{r^2} \tag{2}$$

Motion y component:

$$\frac{\partial}{\partial t}(\rho v) + \frac{1}{r}\frac{\partial}{\partial r}(r\rho u v) + \frac{\partial}{\partial y}(\rho v v) = \frac{1}{r}\frac{\partial}{\partial r}\left(r\mu\frac{\partial v}{\partial r}\right) + \frac{\partial}{\partial y}\left(\mu\frac{\partial v}{\partial y}\right) - \frac{\partial p}{\partial y} - \rho g \tag{3}$$

Energy:

$$\frac{\partial}{\partial t}(\rho T) + \frac{1}{r}\frac{\partial}{\partial r}(r\rho u T) + \frac{\partial}{\partial y}(\rho v T) = \frac{1}{r}\frac{\partial}{\partial r}\left(r\frac{k}{C_p}\frac{\partial T}{\partial r}\right) + \frac{\partial}{\partial y}\left(\frac{k}{C_p}\frac{\partial T}{\partial y}\right) \tag{4}$$

The buoyancy term ρg which appears in the y momentum conservation equation results from the density variation, being obtained in the Boussinesq approximation. This approximation considers an incompressible flow in the whole of the system, except for the buoyancy force term in the vertical flow. In order to determine a mathematical expression of the buoyancy forces, let us consider the density of the fluid, ρ_0, at a temperature T_0. The density is given by

$$\rho = \rho_0 \left[1 - \beta (T - T_0)\right] \tag{5}$$

Details of the derivation of the Boussinesq approximation can be seen in Bernardes [2]. Defining $p' = p - p_0$ and $\beta = 1/T_0$ and introducing these definitions into equation (3), one has

$$\frac{\partial}{\partial t}(\rho v) + \frac{1}{r}\frac{\partial}{\partial r}(r\rho u v) + \frac{\partial}{\partial y}(\rho v v) = \frac{1}{r}\frac{\partial}{\partial r}\left(r\mu\frac{\partial v}{\partial r}\right) + \frac{\partial}{\partial y}\left(\mu\frac{\partial v}{\partial y}\right) - \frac{\partial p'}{\partial y} + g\rho_0\beta(T - T_0) \tag{6}$$

The governing equations, in cylindrical coordinates, can be written in a general form for a generic magnitude ϕ, as

$$\frac{\partial}{\partial t}(\rho\phi) + \frac{1}{r}\frac{\partial}{\partial r}(r\rho u\phi) + \frac{\partial}{\partial y}(\rho v\phi) = \frac{1}{r}\frac{\partial}{\partial r}\left(r\Gamma^{\phi}\frac{\partial \phi}{\partial r}\right) + \frac{\partial}{\partial y}\left(\Gamma^{\phi}\frac{\partial \phi}{\partial y}\right) + S^{\phi} + P^{\phi} \tag{7}$$

The expressions for the source terms S^{ϕ} and P^{ϕ}, and the diffusivity Γ^{ϕ}, for incompressible flow, are given in *table I*.

TABLE I
Values of ϕ, Γ^{ϕ}, P^{ϕ} and S^{ϕ} for the equation in general form.

Equation	ϕ	Γ^{ϕ}	P^{ϕ}	S^{ϕ}
Continuity	1	0	0	0
Motion – r component	u	μ	$-\partial p/\partial r$	$-2\mu u/r^2$
Motion – y component	v	μ	$-\partial p'/\partial y$	$g\,\rho_0\,\beta\,(T - T_0)$
Energy	T	k/C_p	0	0

Figure 2 shows the domain of the solution. The North boundary is formed by the cover and the chimney wall. The values of the cover temperature and of the chimney wall are respectively T_c as T_t. The non-slip condition is imposed on the velocities u and v on this boundary. The South boundary is formed by the ground and the center of the chimney. At the ground level the temperature is T_{sl}. A non-slip condition is imposed on u and v at this boundary. At the center of the chimney a symmetry condition is imposed both for velocity and temperature. The East boundary corresponds to the top of the chimney, being a mass outflow region. A fully developed flow region is imposed on velocity and temperature. The West boundary is the circumference of the cover, where there is mass inflow. On this boundary, the temperature T_0 is maintained. The velocity, unknown initially, is calculated by numerical simulation in a procedure similar to that of Marcondes [3].

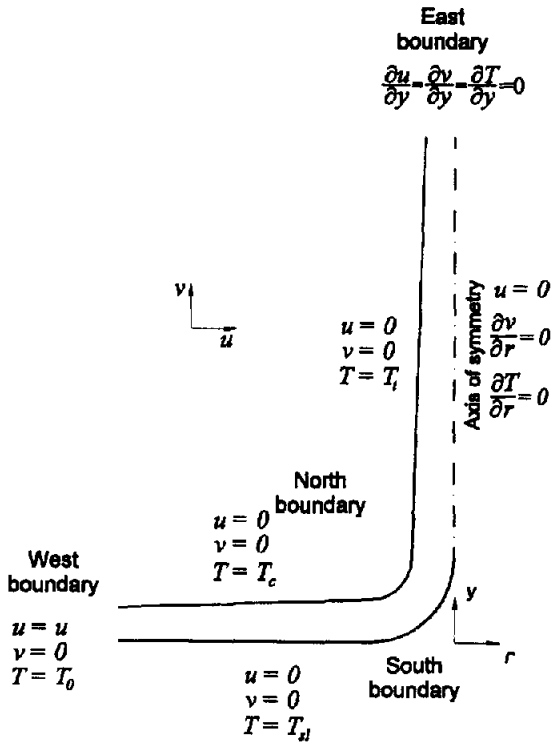

Figure 2. Solution domain and boundary conditions.

3. NUMERICAL METHODOLOGY

For the analysis of the air flow inside the device, the Finite Volumes in Generalized Coordinates Method was used. This methodology allows the study of geometries with different slants of the cover, as well as variant boundary shapes, where the solution can be obtained in a fixed computational domain, independent of the geometry of the real system. The solution of transport equations using generalized coordinates involves the use of two main algorithms: one for the generation of the coordinate system (mesh generation), and the other for the solution of the physical system. A general description of this methodology is given by Maliska [4].

3.1. Coordinate transformation

In this work, we use a system of differential elliptic equations for mesh generation [2] and a method for the coordinate system transformation given by Maliska [4]. In this methodology, for a bidimensional system, the curved coordinates of a point are related to a cylindrical coordinate system by means of two transformation equations, $\xi = \xi(r,y)$ and $\eta = \eta(r,y)$.

The differentials in the transformed domain are given in matricial form by

$$[d^T] = [A][d^T] \quad \text{and} \quad [d^F] = [B][d^F] \tag{8}$$

The metrics are found by comparing $[A]$ to $[B^{-1}]$, thus obtaining

$$\xi_r = J\,y_\eta;\ \xi_y = -J\,r_\eta;\ \eta_r = -J\,y_\xi;\ \eta_y = J\,r_\xi \tag{9}$$

The Jacobian of the transformation is given by

$$J = \begin{vmatrix} \xi_r & \xi_y \\ \eta_r & \eta_y \end{vmatrix} = \xi_r\,\eta_y - \xi_y\,\eta_r = (r_\xi y_\eta - r_\eta y_\xi)^{-1} \tag{10}$$

The length along the coordinate axis is given by

$$\mathrm{d}L_\xi = \sqrt{\alpha}\,\Delta\xi;\ \mathrm{d}L_\eta = \sqrt{\gamma}\,\Delta\eta \tag{11}$$

and the components of the metric tensor are given as

$$\alpha = r_\eta^2 + y_\eta^2;\ \gamma = r_\xi^2 + y_\xi^2;\ \beta = r_\eta r_\xi + y_\xi y_\eta \tag{12}$$

The contravariant velocity components are given by

$$U = u\,y_\eta - v\,r_\eta;\ V = v\,r_\eta - u\,y_\xi \tag{13}$$

In this way, by applying the general transformation described by Valle [5] to the generic equation in cylindrical coordinates, the general transformed equation leads to

$$\begin{aligned}\frac{1}{J}\frac{\partial}{\partial t}(\rho\phi) + \frac{1}{r}\frac{\partial}{\partial \eta}[r\rho\phi V] + \frac{1}{r}\frac{\partial}{\partial \xi}[r\rho\phi U] - \frac{P^\phi}{J} \\ = \frac{1}{r}\frac{\partial}{\partial \eta}\left\{rJ\Gamma^\phi\gamma\frac{\partial\phi}{\partial\eta} - rJ\Gamma^\phi\beta\frac{\partial\phi}{\partial\xi}\right\} \\ + \frac{1}{r}\frac{\partial}{\partial \xi}\left\{rJ\Gamma^\phi\alpha\frac{\partial\phi}{\partial\xi} - rJ\Gamma^\phi\beta\frac{\partial\phi}{\partial\eta}\right\} + \frac{S^\phi}{J}\end{aligned} \tag{14}$$

The expressions for the source terms and the diffusivities of the general transformed equation are given in *table II*.

3.2. Derivation of approximate equations

Conservation equations in a generic variable ϕ written in generalized coordinates in two dimensions, have the form of equation (15) with terms defined in *table II*. On adopting a full implicit formulation, the integration of the equation in time and space, for an elementary volume P, as shown in *figure 3*, results in

$$\begin{aligned}&\frac{M_P\phi_P - M_P^0\phi_P^0}{\Delta t} + \dot{M}_c\phi_e - \dot{M}_w\phi_w + \dot{M}_n\phi_n - \dot{M}_s\phi_s \\ &= \left(D_1\frac{\partial\phi}{\partial\xi} + D_2\frac{\partial\phi}{\partial\eta}\right)_e - \left(D_1\frac{\partial\phi}{\partial\xi} + D_2\frac{\partial\phi}{\partial\eta}\right)_w \\ &+ \left(D_3\frac{\partial\phi}{\partial\eta} + D_4\frac{\partial\phi}{\partial\xi}\right)_n - \left(D_3\frac{\partial\phi}{\partial\eta} + D_4\frac{\partial\phi}{\partial\xi}\right)_x \\ &+ r\,L\,[\widehat{S}^\phi + \widehat{P}^\phi]\,\Delta\xi\,\Delta\eta\end{aligned} \tag{15}$$

TABLE II
Expressions for the source terms and diffusivity coefficients for the general transformed equation.

Equation	ϕ	Γ_ϕ	P^ϕ	S^ϕ
Continuity	1	0	0	0
Motion – r component	u	μ	$y_\eta \frac{\partial p}{\partial \xi} - y_\xi \frac{\partial p}{\partial \eta}$	$-2\mu u / J r^2$
Motion – y component	v	μ	$r_\xi \frac{\partial p}{\partial \eta} - r_\eta \frac{\partial p}{\partial \xi}$	$g \rho_0 \beta (T - T_0)/J$
Energy	T	k/C_p	0	0

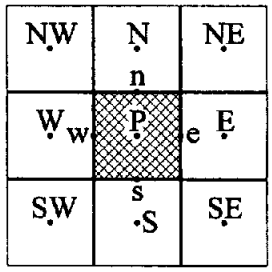

Figure 3. Elementary volume P and its neighbors.

By using the WUDS (*Weighted Upstream Differencing Scheme*) as an interpolation method, and a scheme for storing the variables, then introducing the expressions for ϕ and its derivatives on the boundaries in equation (16), a discretized equation for the elementary volume P is obtained:

$$A_P\phi_P = A_e\phi_E + A_w\phi_W + A_n\phi_N - A_s\phi_S + A_{me}\phi_{NE} + A_{nw}\phi_{NW} + A_{se}\phi_{SE} + A_{sw}\phi_{SW} + B \quad (16)$$

where the coefficients are given by:

$$A_P = \sum A_{NB} + \frac{M_P^0}{\Delta t} \quad (17)$$

$$A_e = -\dot{M}_e\left(\frac{1}{2} - \overline{\alpha}_e\right) + \frac{(D_1\overline{\beta})_e}{\Delta\xi} + \frac{(D_4)_n}{4\Delta\xi} - \frac{(D_4)_s}{4\Delta\xi} \quad (18)$$

$$A_w = \dot{M}_w\left(\frac{1}{2} + \overline{\alpha}_w\right) + \frac{(D_1\overline{\beta})_w}{\Delta\xi} + \frac{(D_4)_s}{4\Delta\xi} - \frac{(D_4)_n}{4\Delta\xi} \quad (19)$$

$$A_n = -\dot{M}_n\left(\frac{1}{2} - \overline{\alpha}_n\right) + \frac{(D_3\overline{\beta})_n}{\Delta\eta} + \frac{(D_2)_e}{4\Delta\eta} - \frac{(D_2)_w}{4\Delta\eta} \quad (20)$$

$$A_s = \dot{M}_s\left(\frac{1}{2} + \overline{\alpha}_s\right) + \frac{(D_3\overline{\beta})_s}{\Delta\eta} + \frac{(D_2)_w}{4\Delta\eta} - \frac{(D_2)_e}{4\Delta\eta} \quad (21)$$

$$A_{ne} = \frac{(D_2)_e}{4\Delta\eta} + \frac{(D_4)_n}{4\Delta\xi} \quad (22)$$

$$A_{se} = -\frac{(D_2)_e}{4\Delta\eta} - \frac{(D_4)_s}{4\Delta\xi} \quad (23)$$

$$A_{nw} = -\frac{(D_2)_w}{4\Delta\eta} - \frac{(D_4)_n}{4\Delta\xi} \quad (24)$$

$$A_{sw} = \frac{(D_2)_w}{4\Delta\eta} + \frac{(D_4)_s}{4\Delta\xi} \quad (25)$$

$$B = r\,L[\widehat{S}^\phi + \widehat{P}^\phi]\Delta\xi\,\Delta\eta + \frac{M_P\phi_P}{\Delta t} \quad (26)$$

The parameter $\overline{\alpha}$ varie between -0.5 and 0.5, and always has the same sign as the velocity; the values of $\overline{\beta}$ vary between 0 and 1.

The pressure terms are evaluated by using central differences, being given by

$$L[\widehat{P}^u] = \left[\frac{P_E - P_P}{\Delta\xi} y_\eta - \frac{P_N + P_{NE} - P_S - P_{SE}}{4\Delta\eta} y_\xi\right] \quad (27)$$

$$L[\widehat{P}^v] = \left[\frac{P_N - P_P}{\Delta\xi} r_\xi - \frac{P_E + P_{NE} - P_W - P_{NW}}{4\Delta\eta} r_\eta\right] \quad (28)$$

and the terms $L[S^\phi]$ are given by

$$L[\widehat{S}^u] = -\frac{2\mu u_P}{J_P r_P^2} \quad (29)$$

$$L[\widehat{S}^v] = -g\rho_0\beta(T_P - T_0) \quad (30)$$

3.3. Application of the boundary conditions

The procedure for the application of boundary conditions in this paper involves the use of fictitious volumes. The equations for these volumes are generated as functions of the existing boundary conditions. These equations have the same form as the equations for internal volumes, being given by

$$A_P\phi_P = A_e\phi_E + B_e, \quad A_P\phi_P = A_w\phi_W + B_w,$$
$$A_P\phi_P = A_n\phi_N + B_n \quad \text{and} \quad A_P\phi_P = A_s\phi_S + B_s$$

representing the West, East, South and North boundaries, respectively.

As shown in *figure 2*, the West boundary is at the periphery of the cover, where the mass flows in. The East boundary is the top of the chimney, where the flow is considered as thermally and hydrodynamically developed. The North boundary is the cover plus ground and the chimney wall. The South boundary consists of ground and the center of the chimney, representing the axis of symmetry.

North Boundary

The two parts of North boundary, the cover and the chimney wall, are impermeable, the prescribed velocities both being zero. In order to comply to this condition in the transformed plane, one must have $u_N = -u_P$, $v_N = 0$ and $V_N = 0$. The cover temperature is represented as T_c while the chimney temperature is T_t. Therefore, the interface temperatures are respectively $T_f = 2\,T_c - T_P$ for the cover, and $T_f = 2\,T_t - T_P$ for the chimney (*figure 4a*).

South boundary

The South boundary is divided into two parts: the ground and the symmetry axis. The ground is impenetrable frontier, with a zero velocity, in which $u_S = u_P$, $v_S = 0$ and $V_S = 0$. The central axis is a symmetry boundary, in which $u_S = u_P$, $v_S = 0$ and $V_S = 0$. At the ground, the temperature is T_{sl} and on the chimney there is a symmetry condition. Therefore, one has $T_f = 2\,T_{sl} - T_P$ for the ground and $T_S = T_P$ for the chimney (*figure 4b*).

East boundary

This is a mass outflow boundary. Its velocity profile attains the fully developed stage. Therefore, a zero derivative condition is applied: $\partial u/\partial y = \partial v/\partial y = 0$, or $u_P = u_E$ and $v_P = v_E$ and $T_P = T_E$ (*figure 4c*).

West boundary

This is a mass inflow boundary. In natural convection problems, the mass flow at the entrance, caused by buoyancy forces, is unknown in the beginning. In this paper, the entrance velocity was initially unknown, being updated at each iteration by the values of the neighboring velocities. This procedure should not be interpreted as being iterative, because the entrance velocity evolves in the same way as the channel interior velocities do. One of the assumptions of Marcondes [3] is that the value of the entrance pressure is kept at zero.

According to this methodology, one has for the West boundary

$$U_P = A_E(u_E y_\eta - v_E r_\eta) + A_N(u_N y_\eta - v_N r_\eta) + A_S(u_S y_\eta - v_S r_\eta) + \frac{\rho_P\, r_P\, \Delta\eta\, \Delta\xi}{\Delta t\, J_P\, A_P}(u_P^\circ y_\eta - v_P^\circ r_\eta) - 2\, r_P \alpha_P \frac{\Delta P}{\Delta\xi}\frac{\Delta\eta^2 \Delta\xi}{A_P} \quad (31)$$

The prescribed temperature is T_0, which means $T_f = 2\,T_0 - T_P$ (*figure 4d*).

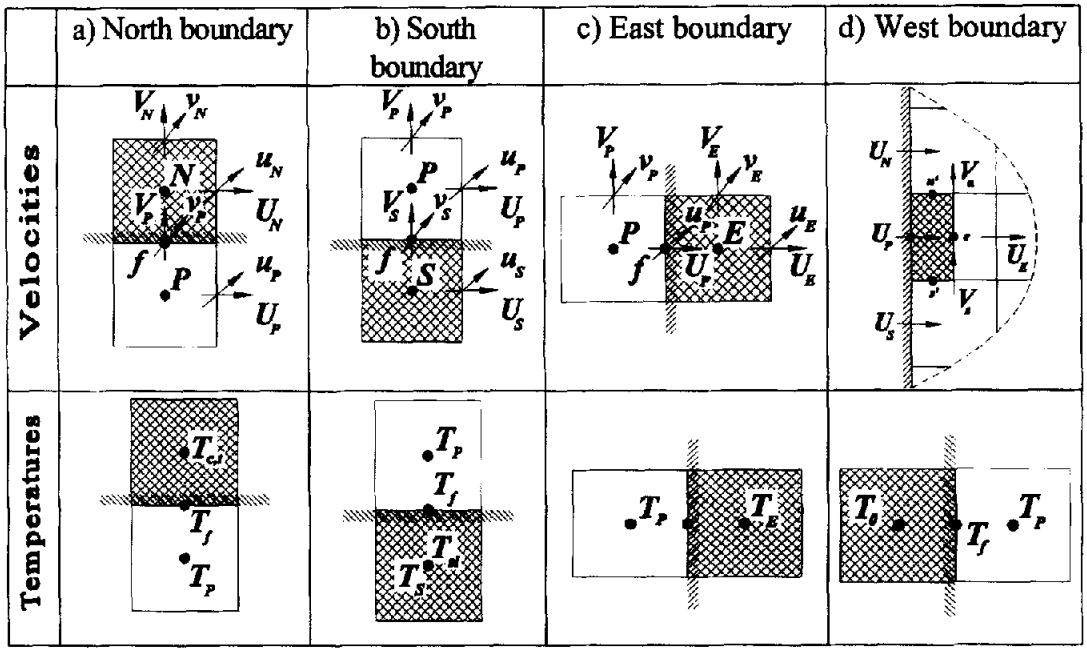

Figure 4. Control volumes for the velocities and temperatures on the boundaries of the transformed plane.

4. RESULTS

In the numerical analysis, the shaping of mesh has obeyed the best distribution of volumes in the domain, with the possibility of refining the details wherever necessary. As an example, *figure 5* shows the mesh detail at the junction, for one of the cases simulated.

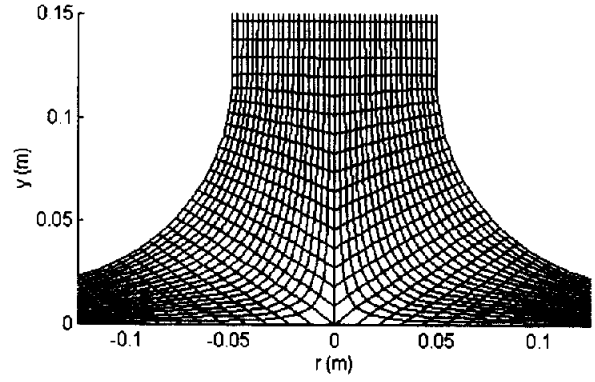

Figure 5. Mesh detail at the junction for one of the geometries studied.

The mesh, a 350×22 volumes arrangement, has proved to be satisfactory, being adopted for most of the cases. Such a refinement was unnecessary in some cases. The natural convection problem between parallel vertical plates was used for the validation of the computational problems. The solutions employed were the following: an analytic solution of the fully developed hydrodynamic flow between two plane plates, as given by Bejan [6], and the numerical solution for the development of thermal and hydrodynamic flow obtained by Bodoia and Osterle [7], which was experimentally validated by Aung et al. [8]. For the last case, the fully developed profiles of temperature and velocity were compared.

In order to study the main thermal and hydrodynamic characteristics of the laminar flow and to evaluate the quality of our numerical methodology, the magnitudes adopted in the simulation were given by the following values: height of the cover at the entrance ($H_{c2} = 0.02$ m); chimney radius at the outlet ($R_{t2} = 0.05$ m); height of the chimney ($H_t = 2$ m); cover radius ($R_c = 1$ m); temperatures ($T_{sl} = 302$ K, $T_c = 300$ K, $T_t = 300$ K, $T_0 = 300$ K), uniformly distributed at the domain boundaries with the geometry given by *figure 6*. It should be noted that these magnitudes do not constitute real conditions of the system, being established only to insure a laminar flow.

Starting from standard geometries (*figure 7*, varied geometries were introduced in the form of five basic configurations (*table III*).

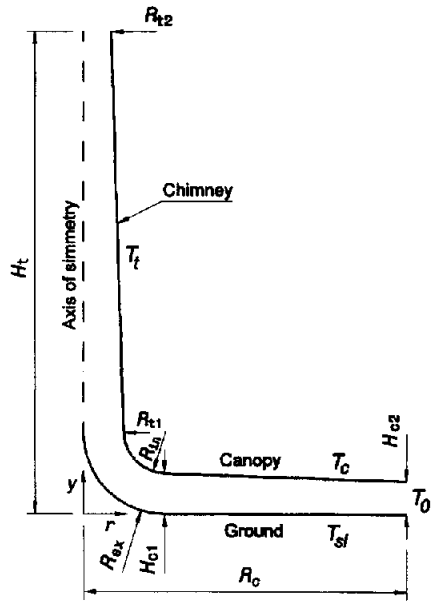

Figure 6. Characteristic geometry.

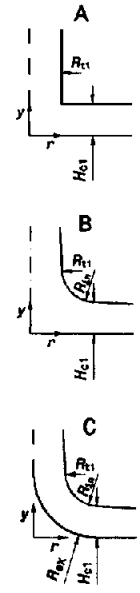

Figure 7. Basic configurations.

Curved junctions originate well-distributed temperature fields, recirculation-free flow (*figures 8* and *9*), as well a higher mass flows (*table III*). Straight junction configurations show recirculations at the base of the chimney (*figure 10*). Curved junctions with a diffusor show no recirculations (*figure 11*). Inclined covers may facilitate the appearance of recirculation patterns similar to Bénard cells. *Figures 12* and *13* show,

TABLE III
Geometric parameters and mass flow for simulated cases.

Case	H_{c1}	R_{t1}	R_{in}	R_{ex}	$\dot{M}$ (kg·s^{-1})
Straith juntion	0.02	0.05	–	–	$8.31 \cdot 10^{-4}$
Curved juntion	0.02	0.05	0.10	–	$1.08 \cdot 10^{-3}$
Slanted junction	0.07	0.05	0.10	–	$1.29 \cdot 10^{-3}$
Conic chimney	0.02	0.10	0.10	–	$1.92 \cdot 10^{-3}$
Curved junction/diffusor	0.02	0.05	0.10	0.12	$1.10 \cdot 10^{-3}$

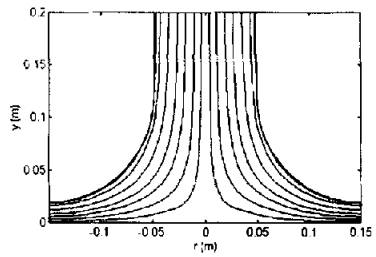

Figure 8. Streamlines for a curved junction.

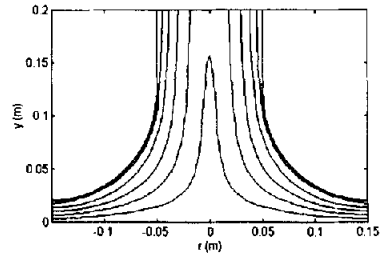

Figure 9. Isothermals for a curved function.

respectively, the formation of such recirculations and their effect on the temperature fields. The conic chimney (*figures 14* and *15*) generates higher mass flows (*table III*), confirming the results of Yan et al. [9].

5. CONCLUSIONS

In this paper a thermo-hydrodynamic analysis for air motion in natural convection, laminar flow and steady state is presented for a radial solar heater with prescribed boundary conditions. The analysis has shown a need for a more detailed investigation of such systems as essential for an ample definition of basic design directions. The literature available is scarce on this type of analyses, as the research mostly concentrates on the evaluation of the global performance of such systems. The adopted methodology was shown to be efficient for the study of localized characteristics of the flow, such as the detection of small recirculations and small temperature gradients.

A few geometric configurations generated perturbations of the flow (recirculations), which reflected on the thermo-hydrodynamic behavior. A conic chimney study corroborated the conclusions of Yan et al. [9], by presenting higher mass flows and higher temperatures at the outlet.

A straight form for the cover–chimney junction gave smaller flows, due to the occurrence of junction flow recirculations. The use of a curved junction allowed higher flows. The introduction of a deflector did not bring major thermal or hydrodynamic improvements.

For the design of real systems, more detailed studies of the geometrical and operational aspects are needed,

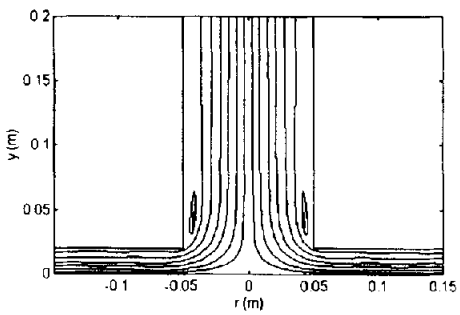

Figure 10. Streamlines for a streight junction.

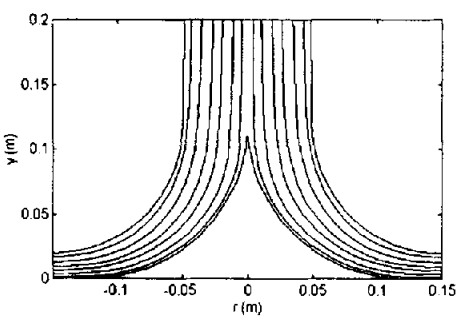

Figure 11. Streamlines for a junction with diffusor.

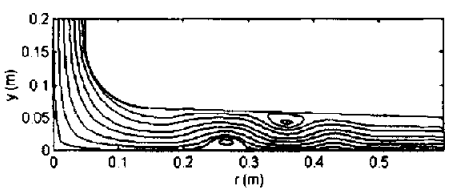

Figure 12. Streamlines for a slanted canopy.

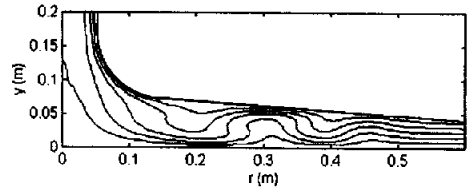

Figure 13. Isothermals for a slanted canopy.

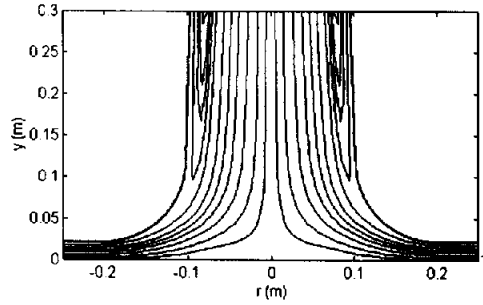

Figure 14. Streamlines for a conical chimney.

involving meteorological conditions and turbulent flow. The numerical methodology presented here is efficient for analyses of such new conditions.

REFERENCES

[1] Schiel W. Schlaich J., Solarthermisches Aufwindkraftwerk, Forum Sonnenenergienutzung BWK 11, 1988, 40.

[2] Bernardes M.A. dos S., Thermal Analysis of a Solar Chimney, M.Sc. Dissertation, Universidade Federal de Minas Gerais, Belo Horizonte, 1997.

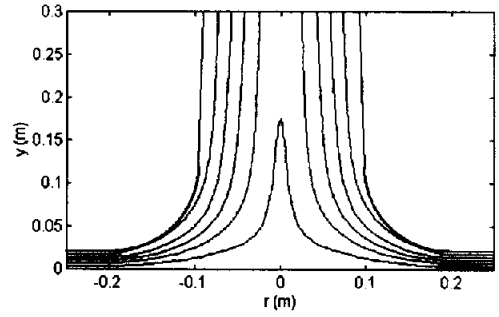

Figure 15. Isothermals for a conical chimney.

[3] Marcondes F., Solução numerica do problema eliptico de convecção natural em canais abertos, M.Sc. Dissertation, Universidade Federal de Santa Catarina, Florianópolis, 1988.

[4] Maliska C.R., Transferência de calor e mecânica dos fluidos computacional, Livros Técnicos e Científicos Editora S.A., Rio de Janeiro, 1995.

[5] Valle R.M., Escoamento laminar em placas de orifício. Análise teórica e experimental em regime permanente e transiente, Thesis, Universidade Federal de Santa Catarina, Florianópolis, 1995.

[6] Bejan A., Convection Heat Transfer, 2nd Ed., John Wiley & Sons, New York, 1984.

[7] Bodoia J.R., Osterle J.F., The development of free convection between heated vertical plates, J. Heat Trans.-T. ASME 84 (1962) 40-44.

[8] Aung W., Fletcher L.S., Sernas V., Development of laminar free convection between vertical flat plates with asymmetric heating, Int. J. Heat Mass Trans. 15 (1972) 2293-2308.

[9] Yan M.Q., Sherif S.A., Kridli G.T., Lee S.S., Padki M.M., Thermo-fluid analysis of solar chimneys, industrial applications of fluid mechanics, ASME FED 132 (1991) 125-130.